Plasma Phys. Control. Fusion **54** (2012) 124041 (7pp) doi:10.1088/0741-3335/54/12/124041

Exponential power spectra, deterministic chaos and Lorentzian pulses in plasma edge dynamics

J E Maggs and G J Morales

Physics and Astronomy Department, University of California, Los Angeles, CA 90095, USA

Received 25 June 2012, in final form 2 September 2012
Published 21 November 2012
Online at stacks.iop.org/PPCF/54/124041

Abstract
Exponential spectra have been observed in the edges of tokamaks, stellarators, helical devices and linear machines. The observation of exponential power spectra is significant because such a spectral character has been closely associated with the phenomenon of deterministic chaos by the nonlinear dynamics community. The proximate cause of exponential power spectra in both magnetized plasma edges and nonlinear dynamics models is the occurrence of Lorentzian pulses in the time signals of fluctuations. Lorentzian pulses are produced by chaotic behavior in the separatrix regions of plasma $E \times B$ flow fields or the limit cycle regions of nonlinear models. Chaotic advection, driven by the potential fields of drift waves in plasmas, results in transport. The observation of exponential power spectra and Lorentzian pulses suggests that fluctuations and transport at the edge of magnetized plasmas arise from deterministic, rather than stochastic, dynamics.

(Some figures may appear in colour only in the online journal)

1. Introduction

Significant experimental and theoretical effort has been devoted to the identification of the origin of the ubiquitous fluctuations observed at the edges of magnetically confined plasmas [1]. While the major thrust in this area arises from magnetic fusion research, because turbulent fluctuations can degrade the performance of confinement devices, the topic is also of interest in space plasma investigations in which enhanced transport across naturally existing sharp boundaries (in temperature, density, magnetic field) can lead to major effects observable by spacecraft and ground-based instruments. The work by Kolmogorov [2] has had a major influence in this subject. In particular, the general prediction of algebraic spectral dependences, made in this pioneering work, has led to the publication of most plasma spectral data in the log–log scale format. Often, piecewise fits are made to extract power-law indices that are compared with the Kolmogorov prediction or with more advanced studies related to avalanche events [3]. Unfortunately, because of the large dynamic range compressed in log–log displays of data, important phenomena, underlying plasma edge turbulence, have been obscured in numerous publications.

Results from two vastly different experiments, involving pressure gradients across the confinement magnetic field in a large plasma column [4], have provided new insight into the general physical processes responsible for edge fluctuations. The insight has led to a picture in which the underlying dynamics is governed by chaotic advection associated with $E \times B$ motion due to drift waves driven by the pressure gradients. Recently, a connection has been established [5] that demonstrates the generality of exponential power spectra, Lorentzian pulses and deterministic chaos at the edges of magnetically confined plasmas of widely different geometry, and operational parameters. This study summarizes the broader body of evidence supporting this conclusion.

Section 2 presents examples of exponential spectra in two major devices, while section 3 identifies Lorentzian pulses in measured time series. Section 4 examines a model of chaotic advection, and section 5 compares the results with experiment. Section 6 presents conclusions drawn from the body of experimental and modeling evidence.

2. Exponential power spectra

It has been evident for some time that the power spectra of fluctuations measured in the edge region of magnetized plasmas have a similar functional form. Pedrosa *et al* [6] quantified this similarity by scaling the time variables of

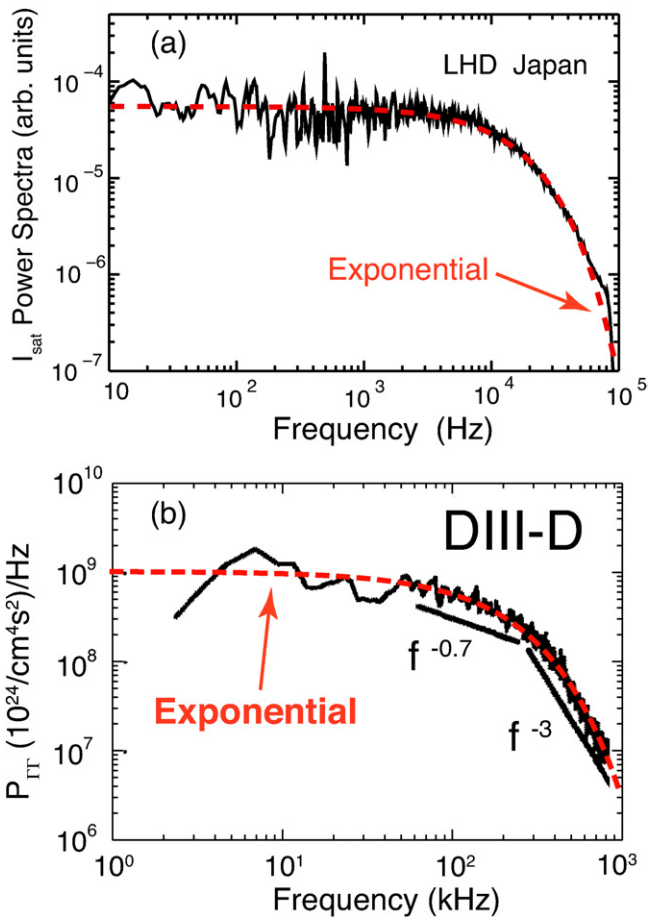

Figure 1. (*a*) Power spectrum of ion saturation current fluctuations observed in the edge of the helical device, LHD (adapted from figure 4(*b*) of [7]), compared with the functional form, $\exp(-2\omega\tau)$ (red dashes). (*b*) Power spectrum of the so-called 'radial turbulent flux' in DIII-D (adapted from figure 3(*a*) of [8]) compared with an exponential. Rhodes *et al* [8] fit the power spectrum, over limited frequency ranges, by two power laws, but the exponential is very close to the observed power spectrum over the entire frequency range.

fluctuation data from the JET tokamak and several stellarators, showing that the power spectra of ion saturation current, floating potential and turbulent radial flux have the same shape. Maggs and Morales [5] pointed out that this shape is described by an exponential function, i.e., the fluctuation power spectra vary as $\exp(-2\omega\tau)$, where τ is a characteristic time scale. This same functional form was observed in the fluctuation power spectra measured in experiments performed in the Large Plasma Device (LAPD), a large linear magnetized device operated at the University of California, Los Angeles (UCLA). Pace *et al* [4] documented in LAPD that fluctuations in ion saturation current, I_{sat}, measured in both a pure temperature filament and at a limiter edge, exhibited exponential power spectra. The pressure gradient scale lengths in these two experiments differed by an order of magnitude, and their origin was different. In the temperature filament study the gradient in pressure was determined by the spatial variation in electron temperature, while in the limiter case it was associated with the variation in plasma density. Figure 1 further illustrates that the observation of exponential spectra applies also to other previously published experiments in two major toroidal devices, not included in the Pedrosa *et al* [6] survey. In figure 1 the red dashed curves labeled 'exponential' have the functional form $\exp(-2\omega\tau)$ and are compared with the experimental observations represented by the black curves, plotted in the original log–log format. From figure 1(*a*) it is seen that the power spectrum of fluctuations in I_{sat} observed in the edge of the helical LHD device [7] exhibits an exponential behavior. Figure 1(*b*) shows the power spectrum of the turbulent radial flux observed in the edge of the DIII-D tokamak by Rhodes *et al* [8]. In [8] the frequency variation of the observed power spectra is compared with a power law of the form $1/f^{\alpha}$; in this display format a power law is a straight line while an exponential exhibits a continuously varying slope. It is argued in [8] that two power laws, $1/f^{0.7}$, in the low-frequency range, and $1/f^{3}$, in the high-frequency range, represent the observations and are consistent with the process of self-organized criticality (SOC). However, the power laws approximate the power spectrum over limited frequency ranges, whereas the exponential is very close to the observed power spectrum over the entire frequency range. This distinction is of fundamental significance because exponential power spectra in the time signals of nonlinear dynamic models indicate the presence of chaotic behavior [9–11], which differs from SOC, in that the former is a deterministic process while the latter is stochastic.

3. Lorentzian pulses

Pace *et al* [4] discovered that exponential fluctuation power spectra observed in the LAPD experiments are caused by the occurrence of Lorentzian-shaped pulses in the I_{sat} signals. Importantly, the average width of the pulses observed in the time series, τ_L, is very close to the time scale, τ, characterizing the exponential power spectra (i.e. $\tau_L \approx \tau$). The close relationship between exponential power spectra and Lorentzian pulses was subsequently verified by Hornung *et al* [13] from data collected in the TJ-K stellarator operated at Stuttgart University. A difference noted between the LAPD results and the TJ-K observations was that, at high frequencies, the TJ-K spectra departed from an exponential dependence given by a single characteristic time, τ. Specifically, at high frequencies, TJ-K spectra display a shallower slope than a pure exponential one (in a log–linear plot). Hornung *et al* [13] demonstrated that, in TJ-K, this departure is due to the distribution of the widths of the Lorentzian pulses observed in the I_{sat} signals.

To more precisely demonstrate the exponential character of the Pedrosa *et al* [6] survey, and to closely connect it to the TJ-K findings, figure 2 shows the data from the I_{sat} power spectra of [6] plotted in a log–linear format rather than the original log–log format. An exponential functional dependence is a straight line in a log–linear format. Figure 2(*a*) compares the power spectrum of an ensemble of artificial time signals (orange color) to the [6] data (various colors). The ensemble of artificial signals used in the comparison comprises 64 signals, each member 1 ms in duration. Each individual

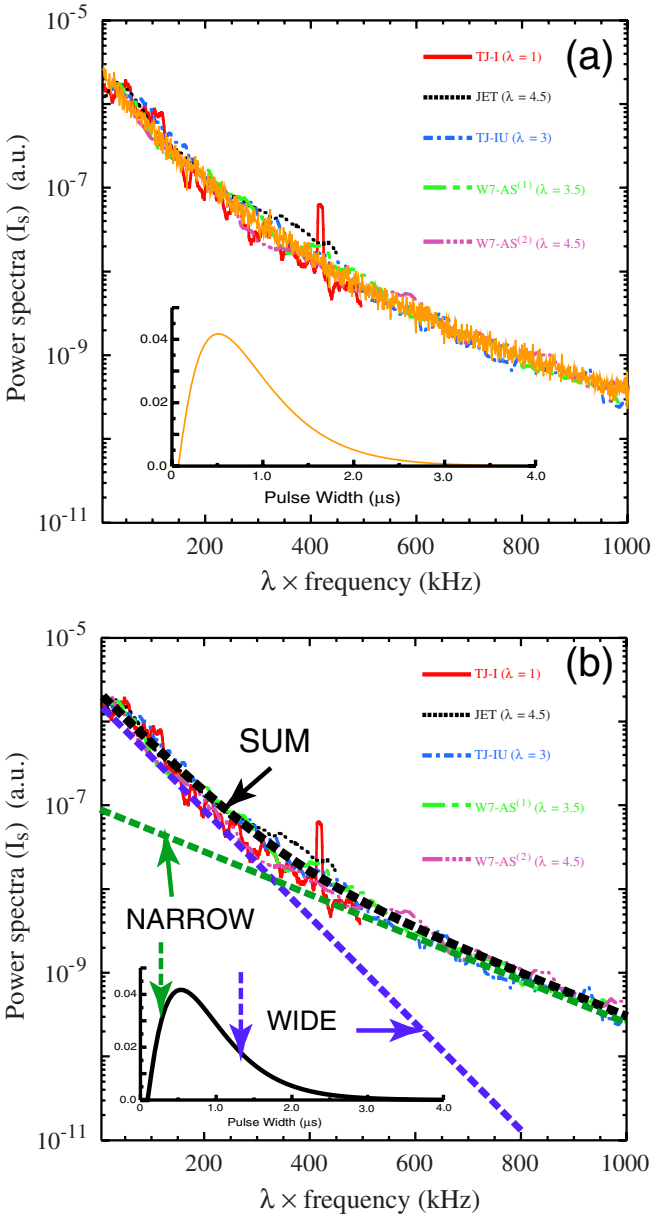

Figure 2. (*a*) Ion saturation power spectra (various colors) from figure 3(*a*) of [6], in a log–linear format, compared with the power spectra of an ensemble of 'artificial' signals constructed from Lorentzian pulses (orange line). The width distribution of the Lorentzian pulses used to construct the 'artificial' signals is shown in the inset. (*b*) The same data in (*a*) fitted by the sum of two exponentials, physically representing two Lorentzian pulse shapes with different characteristic widths. Reused from [6] with permission. Copyright 1999, the American Physical Society.

signal is constructed by adding between 15 and 25 Lorentzian-shaped pulses with randomly chosen center times, amplitudes and widths. The amplitudes are uniformly distributed from −1 to 1, the center times are uniformly distributed over the 1 ms interval, and the width distribution has the form shown in the inset of figure 2(*a*). The distribution used for the artificial signal ensemble is very similar to those reported by Hornung *et al* [13]. Figure 2(*b*) illustrates that a very good fit to the [6] $I_{\rm sat}$ power spectrum can be obtained by adding two exponentials, one representing a wide pulse and the other a narrow pulse. The representative wide pulse determines the slope at low frequencies, while the representative narrow pulse determines the behavior at high frequencies. The two-pulse fit, perhaps, has a physical origin considering $I_{\rm sat}$ is comprised of two physical variables, density and electron temperature.

The variety of pulse shapes observed in various magnetic confinement devices is displayed in figure 3. All of the pulse shapes displayed are obtained by a conditional averaging technique. In this technique, only those pulses whose amplitudes exceed a prescribed threshold are used in the average. All pulses are centered so that their maxima are aligned before the average is taken. This technique helps reduce the distortion in pulse shapes caused by the presence of other fluctuations (such as coherent drift waves). Figure 3(*a*) shows a conditionally averaged $I_{\rm sat}$ pulse from the LAPD limiter edge, gradient experiment with axial field strength 700 G [12]. Figure 3(*b*) is an $I_{\rm sat}$ pulse from the low magnetic field case (720 G) in the TJ-K stellarator [13]. Figure 3(*c*) is an electron temperature pulse from the DIII-D tokamak [14]. Figure 3(*d*) is an $I_{\rm sat}$ pulse from the LHD device [7]. All of the pulse shapes displayed in figure 3 (black curves) are closely fit by a Lorentzian pulse shape (red dashed curves). The observed pulses in panels (*a*), (*c*) and (*d*) are fit by a curve labeled 'skewed' Lorentzian. The 'skewed' Lorentzian is a basic Lorentzian pulse with a left–right asymmetry. A skewed Lorentzian pulse is defined by its Fourier transform

$$\tilde{L}(\omega) = \exp\left(-|\omega|t + \mathrm{i}\left[\frac{2s}{\pi}|\omega|\tau\,\ln(|\omega|\tau) + \omega t_0\right]\right). \qquad (1)$$

In equation (1) the pulse width is given by τ, the location of the peak is at $t = t_0$ and 's' determines the skewness of the pulse. A positive value of 's' means that the pulse amplitude increases slower before the peak than after, i.e. the pulse is 'skewed' to the left. Note that neither the pulse location (t_0) nor the skewness (s) affects the power spectrum of a single Lorentzian pulse, because both of these terms appear as phase factors in the Fourier amplitude. Thus, the power spectrum (the square of absolute value of the Fourier amplitude) associated with a single, skewed pulse of width, τ, is the same as a single Lorentzian pulse of width, τ, $|\tilde{L}(\omega)|^2 = \exp(-2\omega\tau)$. For a train of Lorentzian pulses, however, the power spectrum is affected by the skewness because of phase interference effects. The distribution of pulse widths is also important in determining the form of the power spectrum of a train of pulses, as discussed at length in [4].

4. Chaotic advection

Since Lorentzian pulses are the proximate cause of exponential power spectra, it is important to understand the dynamic process that results in time traces with a Lorentzian shape. Maggs and Morales [15] showed that Lorentzian pulses arise from chaotic dynamics near the separatrix regions of potential flow fields and the limit cycle regions of nonlinear dynamic models. A 2D bifurcation in the Cartesian (x, y) space, the Lorentzian bifurcation, is introduced in [15] that represents the dynamic behavior of $E \times B$ orbits in the electric potential fields produced by the linear superposition of two cylindrical

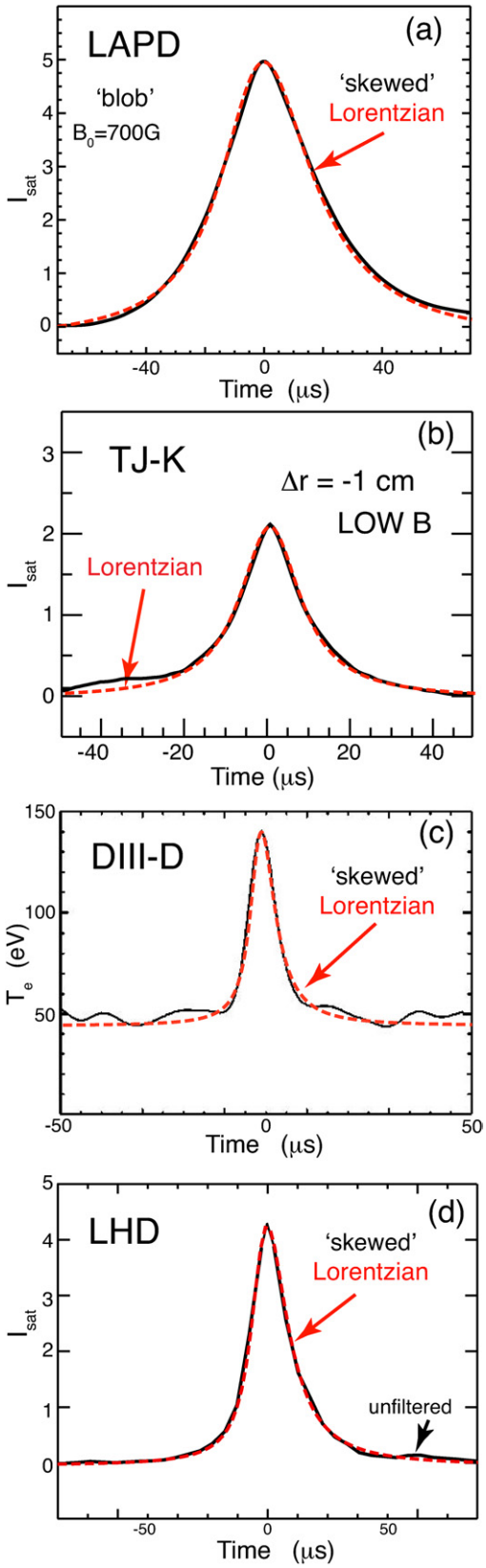

Figure 3. 'Conditionally averaged' pulse shapes (black solid curves) observed in four, vastly different, plasma devices compared with Lorentzians (dashed red curves): (*a*) linear LAPD (adapted from figure 4(*a*) of [12], with permission. Copyright 2006, American Institute of Physics.), (*b*) the TJ-K stellarator (adapted from figure 4 of [13], with permission. Copyright 2011, American Institute of Physics.), (*c*) the DIII-D tokamak (adapted from figure 7(*a*) of [14], with permission. Copyright 2001, American Institute of Physics.) and (*d*) the helical LHD (adapted from figure 9(*a*) of [7]). The term 'skewed' Lorentzian is explained in the text.

waves with different azimuthal mode numbers. The Lorentzian bifurcation has closed-form solutions whose y-displacements, $y(t)$, are, roughly speaking, either the sum of Lorentzian pulses, or the difference in Lorentzian pulses. Such dynamical behavior in the presence of a linear gradient gives rise to time signals that consist of Lorentzian pulses. When the parameters of the Lorentzian bifurcation are modulated in time, the behavior becomes chaotic. The solutions become trains of pulses of varying number and pulse width depending on the amplitude and frequency of the modulation. Such behavior is called 'deterministic chaos' because the solutions to the motion are given by a known set of differential equations that can, in principle, be solved exactly. Yet the solutions in chaotic systems are very sensitive to initial conditions. A given known solution for one starting point is not predictive of the behavior of solutions starting in the immediate vicinity of that point.

The linear superposition of two cylindrical waves could result in $E \times B$ flows that become chaotic. Such 'chaotic advection' can result in plasma transport because chaotic motion is irreversible. To test these ideas, a chaotic advection model is used to study temperature transport in a narrow temperature filament, such as that investigated experimentally in LAPD [4, 16, 17]. In the model, the electric potential is given by the linear superposition of two radially localized cylindrical waves with azimuthal mode numbers, $m = 1$ and $m = 6$ with the corresponding radial Bessel function behavior, $J_1(k_{(1)\perp}r)\mathrm{e}^{-\alpha r}$ and $J_6(k_{(6)\perp}r)\mathrm{e}^{-\alpha r}$, as described in detail by Shi *et al* [18]. This potential structure is based on experimental observations of drift waves, but is not self-consistently derived from the pressure profile. In [18] the transport model considered consisted of both classical heat conduction (arising from Coulomb collisions) and chaotic $E \times B$ advection. The ratio between the advection term and the conduction term in the transport equation is referred to as the Péclet number, which is about 30 for the results reported in [18]. The model system was found to produce transport and Lorentzian pulses consistent with experimental observations.

The inclusion of classical heat conduction in the model somewhat obscures the role of chaotic advection in the transport process. In order to isolate the effects of chaotic advection, a pure advection model of heat transport, in which the Péclet number is formally infinite (heat conduction is assumed to be zero), is applied to the temperature filament model. Solutions are obtained by integrating initial conditions along the Lagrangian trajectories, or orbits. The Lagrangian orbits exhibit chaotic behavior when the amplitudes of the two linearly superposed cylindrical modes are large enough. Chaotic behavior requires the presence of the two modes, one mode alone will not produce chaotic behavior. In the chaotic advection model the frequency of both modes is chosen, consistent with experimental observations, to be 50 kHz. The amplitude of the $m = 1$ mode, initially zero, is increased slowly (proportional to a hyperbolic tangent function) over four wave periods to its final value, and then the $m = 6$ mode amplitude is increased in the same fashion once the $m = 1$ mode is at full amplitude. In the results reported here, the final mode amplitude is 0.2 V, and chaotic behavior is observed to onset when the $m = 6$ mode is above about 0.1 V, half its

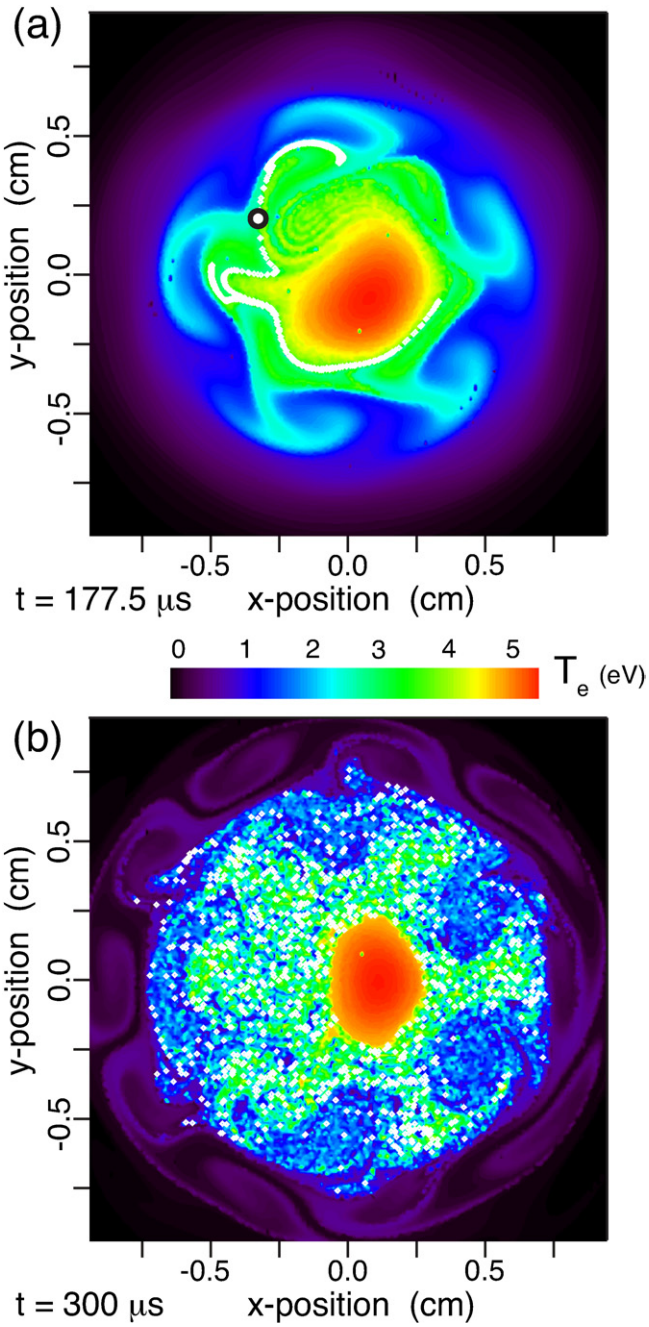

Figure 4. Effect of chaotic advection illustrated by plotting the endpoints of 1024 Lagrangian trajectories at two times, superimposed on color contours of the corresponding temperature profiles. (*a*) Initial positions of the trajectories indicated by the small black circle at about ten o'clock. The white symbols are the trajectory end points a $t = 177.5\,\mu$s, a time before chaotic behavior occurs. (*b*) Trajectory endpoints at $t = 300\,\mu$s. The chaotic spatial distribution is evident.

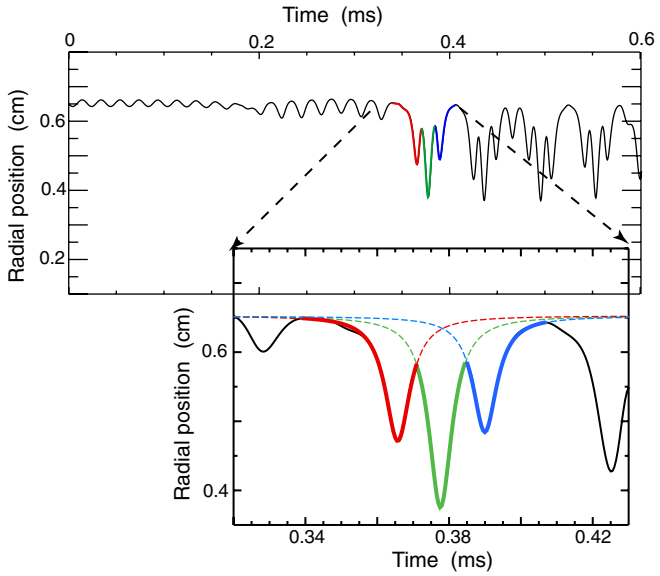

Figure 5. Radial position of a chaotic Lagrangian orbit shown as a function of time. A segment of the trajectory is highlighted in red, green and blue and presented in an expanded view. The colored portions of the expanded trajectory are shown to follow individual Lorentzian-shaped curves.

final amplitude. The initial temperature profile is assumed to be azimuthally symmetric with a Gaussian radial shape with radial scale length 0.3 cm and a peak temperature of 5 eV.

Figure 4 illustrates the effects of chaotic advection. Contours of temperature computed along a 256 × 256 grid of Lagrangian orbits are shown in figure 4(*a*) together with the end points of a select group of such orbits. The select group of orbits is distinct from the orbits used to compute the temperature. The black circle at ten o'clock in panel (*a*) represents the initial positions of 1024 Lagrangian $E \times B$ trajectories, and the white symbols (small squares) are the end points of the same set of trajectories at a time before the onset of chaotic behavior, $t = 177.5\,\mu$s. At this time the temperature contours exhibit complex, but connected, spatial structure. The select group of orbits is also highly distorted, but clearly connected. If the initial group of orbits is considered to delineate a 'blob' of fluid, the blob is highly distorted at $t = 177.5\,\mu$s, but still identifiable as a single connected blob. This situation changes dramatically as the amplitude of the $m = 6$ mode continues to increase. As shown in figure 4(*b*), the temperature contours exhibit an overall large scale structure broken up into many fine scale features. The fine scale features are a result of chaotic advection. The endpoints of the orbits shown in panel (*b*) cover much of the calculation plane with no discernable order. This is the nature of chaos. Neighboring points move along trajectories that diverge from each other.

Details of the radial position, as a function of time, of one particular chaotic orbit are shown in figure 5. This orbit can be used to demonstrate the mechanism by which Lorentzian-shaped pulses are produced in the time signals of the temperature. The orbit begins at a radial position of 0.65 cm, about 2 scale lengths from the center of the temperature filament. Initially, when the amplitude of the $m = 6$ mode is small ($t < 175\,\mu$s), the orbit is oscillatory, no chaotic behavior is apparent and no transport occurs. After $175\,\mu$s the orbit begins to show signs of distortion, chaotic behavior begins to become observable. After $350\,\mu$s chaotic behavior in this particular orbit is obvious, as illustrated by the portion of the curve highlighted in color and expanded in the inset. The sequence of three negative radial excursions (red, green blue) is shown to follow Lorentzian-pulse shapes. Each dashed curve in the inset is a Lorentzian pulse. When

the dashed curve coincides with the Lagrangian trajectory, it becomes solid. It is clear that the trajectory over this time period is composed of a sequence of pieces of three Lorentzian pulses. If the average temperature in the radial region covered by the trajectory (0.35–0.65 cm) has an approximately, linear radial variation, that is, $T_e(r) = T_e(r_0) + a(r - r_0)$, then the temperature fluctuation signal, measured at a fixed radial location through which this particular trajectory passes, will have the same Lorentzian pulse shape as the trajectory.

5. Comparison with experiment

The chaotic advection model is implemented by choosing a time dependence for the mode amplitudes and then calculating, by fourth-order Runge–Kutta integration, the spatial locations $[X(t),\ Y(t)]$ of a set of trajectories with initial positions situated on a 256 × 256 rectangular grid with equal spacing, spanning a 2 cm × 2 cm area. The initial, Gaussian-shaped temperature profile is centered in the calculation grid. The temperature profile is computed at later times from the Lagrangian trajectories. In the simplest case of no source or loss term, the initial temperature is simply advected along each orbit, $T_e(X(t), Y(t)) = T_e(X(0), Y(0))$. The resulting temperature values at time, t, are transferred to the 256 × 256 rectangular grid by assigning the temperature at each trajectory location at time, t, to neighboring grid points in an 'area weighted' fashion. In this manner the temperature value as a function of time is obtained for each grid point. The results of such a procedure are displayed as contours in figure 4, for two representative times.

The results of the chaotic advection model can be directly compared with experimental results by inserting a 'synthetic probe' into the calculation plane of the model. The 'probe' is comprised of a set of neighboring calculation grid points, whose size mimics the probes used in collecting the experimental data. A typical probe size used in data collection is 2 mm × 1 mm, which roughly corresponds to a set of 12 × 6 grid points in the 256 × 256 calculation grid. The 'probe' time signal is taken to be the sum of all the time signals at each point in the 12 × 6 grid. In the experiment, computed quantities, such as the fluctuation power spectrum, are averaged over an ensemble of signals. In the model, signals are collected from different spatial locations, and computed quantities are averaged over these locations.

Figure 6 presents a comparison between experimental and model results. The fluctuation power spectra are displayed in figure 6(*a*), and it is apparent that the two are very similar. The model shows temperature fluctuations and the experiment, strictly speaking, measures fluctuations in the ion saturation current, but, due to the experimental design, these fluctuations are almost entirely temperature fluctuations.

Both power spectra show a 'line' component that consists of a fundamental mode and a few harmonics. In the experimental spectrum, the 'line' at about 7 kHz is caused by the excitation of a thermal diffusion wave at the center of the temperature filament [19], and this phenomenon is not included in the advection model. The peaks in the experimental power spectrum at higher frequencies (above 20 kHz) arise

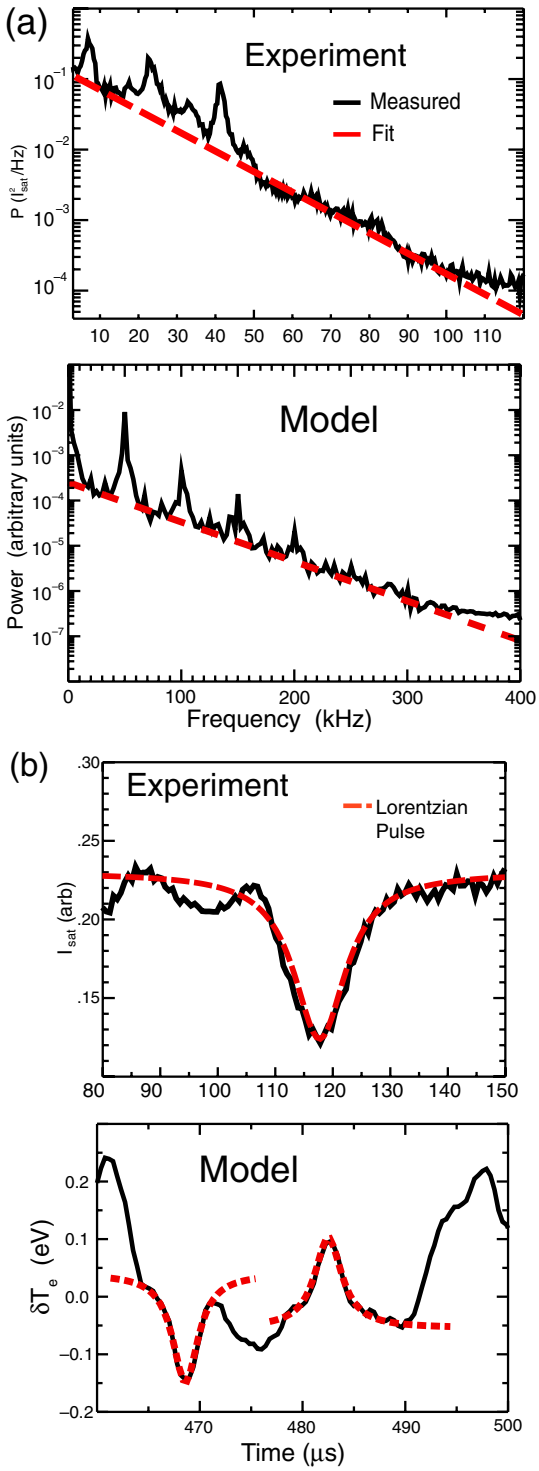

Figure 6. Results from the chaotic advection model compared with the corresponding results from the temperature filament experiment in the linear device LAPD [4]. (*a*) Power spectra and (*b*) Lorentzian pulses in the time signals. The width of the Lorentzian pulses shown in (*b*), experiment: $\tau = 5\,\mu$s, and model: $\tau = 1.5\,\mu$s, is the same characteristic time associated with the dashed, straight red lines ($\exp(-2\omega\tau)$) in (*a*).

from drift waves in the gradient region of the temperature filament. Only drift waves are included in the chaotic advection model, and their influence is readily apparent in the 'line' feature of the model power spectrum. Accompanying the 'line'

features in both power spectra is an exponential 'baseline' that arises from the occurrence of Lorentzian pulses in the time signal data, as shown in figure 6(*b*). The black traces are the time signals, and the red dashed lines are Lorentzian pulses whose power spectra are shown as the red dashed lines in panel (*a*). Clearly, the pulses observed in the time signals, for both the experiment and model, are consistent with the power spectra. While the morphology of the power spectra and time signals from the model and experiment agree, the absolute time scales differ. The frequency span displayed in panel (*a*) is larger for the model because the pulses observed in the model are narrower than those observed in the experiment. Narrower pulses contain more power at high frequencies. This is consistent with the much larger Péclet number of the model (formally infinite) as compared with the experiment ($P_e = 30$). The pulses observed in the model described in [18], which included heat conduction along with chaotic advection, have widths similar to those observed in the experiments.

6. Conclusions

Exponential fluctuation power spectra are observed in a wide variety of plasma devices: tokamaks, stellarators, helical and linear machines. The exponential character of the power spectrum is due to Lorentzian-shaped pulses in time signals of observed quantities. Various techniques allow for the extraction of Lorentzian-shaped pulses from time signals so that their properties can be cataloged. Importantly, the observed distribution of pulse widths is consistent with the power spectra obtained from the time signals containing the extracted pulses. Such a relationship cannot be established for any other pulse shape. The intimate connection between exponential power spectra and Lorentzian pulses arises from the dynamics of deterministic chaos, which can lead to transport because of its irreversible nature. The observation of exponential fluctuation power spectra and conditionally averaged Lorentzian-shaped pulses at the edges of magnetized plasma devices, the demonstrated consistency, in a subset of these devices, of exponential spectra and Lorentzian pulses contained in the time signals giving rise to those spectra, and the intimate connection between deterministic chaos and exponential power spectra, strongly suggests that transport at the edge of magnetized plasmas results from a deterministic and not a stochastic process.

Acknowledgments

This work was performed under the auspices of the BAPSF at UCLA funded under a DOE/NSF cooperative agreement (DOE: DE-FC02-07ER54918, NSF: PHY-0531621), and by DOE Grant No SC0004663.

References

[1] D'Ippolito D A, Myra J R and Zweben S J 2001 *Phys. Plasmas* **18** 060501
[2] Kolmogorov A 1941 *Dokl. Akad. Nauk SSSR* **32** 16
[3] Bak P, Tang C and Wiesenfeld K 1988 *Phys. Rev.* A **38** 364
[4] Pace D C *et al* 2008 *Phys. Plasmas* **15** 122304
[5] Maggs J E and Morales G J 2011 *Phys. Rev. Lett.* **107** 185003
[6] Pedrosa M A *et al* 1999 *Phys. Rev. Lett.* **82** 3621
[7] Dewhurst J M *et al* 2008 *Plasma Phys. Control. Fusion* **50** 095013
[8] Rhodes T L *et al* 1999 *Phys. Lett.* A **253** 181
[9] Ohtomo N *et al* 1995 *J. Phys. Soc. Japan* **64** 1104
[10] Frisch U and Morf R 1981 *Phys. Rev.* A **23** 2673
[11] Sigeti D E 1995 *Physica* D **82** 136
[12] Carter T A 2006 *Phys. Plasmas* **13** 010701
[13] Hornung G *et al* 2011 *Phys. Plasmas* **18** 082303
[14] Boedo J A *et al* 2001 *Phys. Plasmas* **8** 4826
[15] Maggs J E and Morales G J 2012 *Phys. Rev.* E **86** 015401
[16] Burke A T, Maggs J E and Morales G J 2000 *Phys. Plasmas* **7** 544
[17] Burke A T, Maggs J E and Morales G J 2000 *Phys. Plasmas* **7** 1397
[18] Shi M *et al* 2009 *Phys. Plasmas* **16** 062306
[19] Pace D C *et al* 2008 *Phys. Rev. Lett.* **101** 035033